# Possible roles for Munc18-1 domain 3a and Syntaxin1 N-peptide and C-terminal anchor in SNARE complex formation

Shu-Hong Hu[a,1], Michelle P. Christie[a,1], Natalie J. Saez[a], Catherine F. Latham[a,b,3], Russell Jarrott[a], Linda H. L. Lua[c], Brett M. Collins[a], and Jennifer L. Martin[a,2]

[a]Institute for Molecular Bioscience, Division of Chemistry and Structural Biology, [b]Queensland Brain Institute, and [c]Protein Expression Facility, The University of Queensland, Brisbane, Queensland 4072, Australia

Edited* by Thomas C. Südhof, Stanford University School of Medicine, Palo Alto, CA, and approved November 24, 2010 (received for review December 23, 2009)

**Munc18-1 and Syntaxin1 are essential proteins for SNARE-mediated neurotransmission. Munc18-1 participates in synaptic vesicle fusion via dual roles: as a docking/chaperone protein by binding closed Syntaxin1, and as a fusion protein that binds SNARE complexes in a Syntaxin1 N-peptide dependent manner. The two roles are associated with a closed–open Syntaxin1 conformational transition. Here, we show that Syntaxin N-peptide binding to Munc18-1 is not highly selective, suggesting that other parts of the SNARE complex are involved in binding to Munc18-1. We also find that Syntaxin1, with an N peptide and a physically anchored C terminus, binds to Munc18-1 and that this complex can participate in SNARE complex formation. We report a Munc18-1–N-peptide crystal structure that, together with other data, reveals how Munc18-1 might transit from a conformation that binds closed Syntaxin1 to one that may be compatible with binding open Syntaxin1 and SNARE complexes. Our results suggest the possibility that structural transitions occur in both Munc18-1 and Syntaxin1 during their binary interaction. We hypothesize that Munc18-1 domain 3a undergoes a conformational change that may allow coiled-coil interactions with SNARE complexes.**

membrane trafficking | protein–peptide interaction | protein–protein interaction | Sec/Munc protein

Sec/Munc (SM) and soluble NSF attachment protein receptor (SNARE) proteins play fundamental roles in regulating membrane traffic (1–3). The cognate interacting partners comprising the SM protein Munc18-1 and the SNARE protein Syntaxin1 (Sx1) are of special importance to human physiology because they regulate synaptic vesicle-mediated neurotransmitter release (4). Two alternate binding modes have been described for this pair of proteins. One mode involves Munc18-1 interacting with "closed" Sx1, in which the SNARE H3 helical motif is sequestered by the three Habc helices of Sx1 to form a four-helix bundle (5, 6) (Fig. 1). This closed binding mode is consistent with a negative regulatory role for Munc18-1 because the SNARE H3 helix in closed Sx1 is unable to interact with SNARE partners to form the complexes that drive vesicle fusion (7) (Fig. 1*A*). However, the closed binding mode of Syntaxin is not universal and may be a specialization of regulated exocytosis (8). A second binding mode, which likely underpins a general function of SM proteins, occurs when Sx1 is in an "open" conformation (i.e., when the H3 helix is separated from the Habc helices) in the SNARE ternary complex (9, 10) (Fig. 1*A*). This binding mode is dependent on the very N-terminal 10 residues of Sx1, the N peptide. This second mode is consistent with a positive regulatory role for Munc18-1, because SNARE ternary complex formation is required for vesicle fusion. The N-peptide interaction has been characterized structurally for the highly homologous protein pair of Munc18-3 and Syntaxin4 (Sx4) (11), which regulate trafficking of the insulin-stimulated glucose transporter GLUT4 in muscle and fat cells (12).

Munc18 proteins contribute to specificity of SNARE-mediated vesicle fusion in that Munc18-1 interacts with Sx1 and not Sx4, and vice versa for Munc18-3 (13). However, the critical residues of the Sx4 N peptide that interact with Munc18-3 (Asp3, Arg4, Thr5, and Leu8) are conserved between Sx1 and Sx4, suggesting that the N-peptide interaction may not select for cognate Munc18 interactions (11).

Here, we confirm by isothermal titration calorimetry (ITC) that Munc18-1 does not discriminate significantly between Sx1 and Sx4 N peptides. We also show by X-ray crystallography that the N peptide adopts the same binding conformation and forms similar interactions whether it is bound to cognate or noncognate Munc18 partners. The structure of N-peptide bound rat Munc18-1 adopts an extended domain 3a conformation that may preclude closed Sx1 binding yet remain compatible with binding open Sx1 and SNARE complexes. Extended domain 3a conformations have been observed in all other SM protein structures, except that of rat Munc18-1 bound to closed Sx1. Our analysis of the structures and sequences of SM proteins, together with preliminary circular dichroism (CD) spectroscopy data, suggests that domain 3a may form coiled-coil interactions with SNARE complexes. Finally, we present a speculative model suggesting how Munc18-1 interaction with Sx1 might lead to SNARE complex formation.

## Results

**Sx1 Bound to Munc18-1 Can Form SNARE Complexes.** The Sx1 N peptide has been shown to be important for Munc18-1 binding to SNARE complexes and for membrane fusion (9, 10, 14, 15). However, the recent work of Burkhardt et al. (5) suggested that when bound to Munc18-1, the N peptide inhibits Sx1 interaction with SNARE partner proteins. We had previously shown that the Sx4 N peptide assists SNARE complex formation in the presence of Munc18-3 (16). We wondered whether these conflicting results might be a consequence of experimental design. For our Sx4 experiments (16) we used Sx4 immobilized at its C terminus, whereas Burkhardt et al. performed experiments with Sx1 free in solution (5). We therefore performed pulldown experiments with Sx1 immobilized at the C terminus and found that it binds

Author contributions: S.-H.H., M.P.C., C.F.L., L.H.L.L., B.M.C., and J.L.M. designed research; S.-H.H., M.P.C., N.J.S., R.J., and J.L.M. performed research; S.-H.H., M.P.C., B.M.C., and J.L.M. analyzed data; and S.-H.H., M.P.C., and J.L.M. wrote the paper.

The authors declare no conflict of interest.

*This Direct Submission article had a prearranged editor.

Data deposition: Coordinates and structure factors for the Munc18-1–Sx4 N-peptide complex and the newly refined Munc18-3–Sx4 N-peptide complex have been deposited in the Protein Data Bank, www.pdb.org (PDB ID codes 3PUJ and 3PUK, respectively).

[1]S.-H.H. and M.P.C. contributed equally to this work.

[2]To whom correspondence should be addressed. E-mail: j.martin@imb.uq.edu.au.

[3]Present Address: Department of Biological Science, Columbia University, New York, NY, 10027.

This article contains supporting information online at www.pnas.org/lookup/suppl/doi:10.1073/pnas.0914906108/-/DCSupplemental.

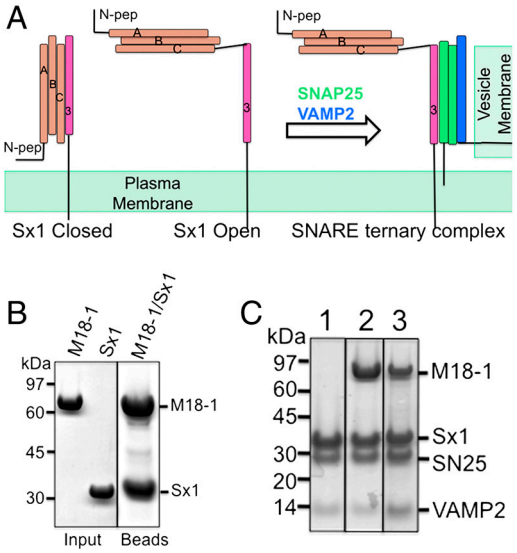


**Fig. 1.** Munc18-1 interaction with Sx1. (*A*) Sx1 Conformations. Sx1 is a helical protein comprising an N peptide (residues 1–10; labeled N-pep), a 3-helical N-terminal domain termed Habc (helices labeled A, B, and C) linked to a SNARE helix H3 (labeled 3) that is tethered to the plasma membrane at the C terminus by a transmembrane region. In the closed Sx1 conformation, the H3 helix interacts with the Habc domain and is unavailable to interact with SNARE partner proteins SNAP25 and VAMP2 (also called Synaptobrevin). When Sx1 adopts an open conformation, the H3 SNARE motif is available to interact with SNARE partner proteins SNAP25 (two helices, green, attached to the plasma membrane via cysteine palmitoylation) and VAMP2 (blue, tethered to the vesicle membrane by a transmembrane region at its C terminus) to form the SNARE ternary complex in a process that drives vesicle fusion. Munc18-1 is known to interact with the closed conformation of Sx1 and with the SNARE ternary complex; the latter interaction is dependent on the Sx1 N peptide. (*B*) Sx1-His–Munc18-1. Sx1-His immobilized on resin forms a complex with Munc18-1. (*C*) Sx1 bound to Munc18-1 participates in SNARE complex formation. Sx1 immobilized on resin by a C-terminal His tag was used alone or in complex with Munc18-1 (*B*) to investigate the formation of SNARE complex. Lane 1 shows the formation of SNARE ternary complex (Sx1/SNAP25/VAMP2) in the absence of Munc18-1; lane 2 shows that preformed Munc18-1–Sx1 complex also interacts with SNAP25 and VAMP2. For comparison, lane 3 shows the relative amounts of these proteins when Munc18-1 is incubated with preformed SNARE complex.

Munc18-1 (Fig. 1*B*); this complex was then incubated with SNAP25 and VAMP2 to explore whether the Munc18-1–Sx1 complex could participate in SNARE complex formation (Fig. 1*C*). Using this approach, SNAP25 and VAMP2 interact with immobilized Munc18-1–Sx1 complex. The relative levels of Munc18-1, Sx1, SNAP25, and VAMP2 on the resin appear to be similar to those produced by incubation of preassembled SNARE ternary complex with Munc18-1 (Fig. 1*C*). This evidence supports the notion that, under the conditions we used, the preassembled heterodimer of Munc18-1–Sx1 may participate in SNARE complex formation, and that neither Munc18-1 nor the presence of the Sx1 N peptide appear to significantly inhibit SNARE complex formation.

**Munc18 Proteins Bind Cognate and Noncognate N Peptides with Similar Affinity.** We measured the binding affinity of Sx1 and Sx4 N peptides for Munc18-1 and Munc18-3 using ITC. Our results show that the Munc18-1 and Munc18-3 proteins interact with their cognate partner N peptides, Sx4 and Sx1, respectively, with favorable enthalpies and dissociation constants, $K_d$, in the micromolar range (Table 1 and Fig. S1). We also found that the interaction between Munc18-1 and the noncognate Sx4 N peptide is of a similar affinity to its interaction with cognate Sx1 N peptide, showing that Munc18-1 does not discriminate significantly between the Sx1 and Sx4 N peptides. Overall, these results indicate that although Munc18-3 binds Syntaxin N peptides 3–20 times more tightly than Munc18-1 binds the same N peptides, both Munc18-1 and Munc18-3 can interact with cognate and noncognate N peptides with micromolar affinities.

**N Peptide Forms Similar Interactions with Munc18-1 and Munc18-3.** To confirm that N peptides interact similarly with cognate and noncognate Munc18 proteins, we determined the crystal structure of Munc18-1 in complex with noncognate Sx4 N peptide (Fig. 2 and Table S1) and compared the binding mode with that of the Sx4 N peptide in complex with its cognate partner, Munc18-3 (Fig. 2 and Fig. S2).

The Munc18-1:Sx4 N-peptide crystal structure has two complexes (A:C and B:D) in the asymmetric unit. In these complexes, the Sx4 N peptide forms 7 hydrogen bonds and 61–73 van der Waals (VdW) contacts with Munc18-1. By comparison, when the same N peptide interacts with Munc18-3 it forms 7–9 hydrogen bonds and 77–110 VdW contacts. In both Munc18-1 and Munc18-3, hydrogen bonds are formed to Sx4 N-peptide residues Arg2, Asp3, Arg4, Thr5, and Arg9, and VdW interactions are formed with these residues and with Leu8. The fewer hydrogen bond and VdW interactions correlate with the weaker $K_d$ value of the Sx4 N peptide for Munc18-1 compared with Munc18-3, providing a molecular basis for its reduced binding affinity.

The binding conformation and hydrogen bonds are conserved in the Munc18-1:Sx4 N peptide and Munc18-3:Sx4 N-peptide complexes (Fig. S2 and Table S2). Taken together, these findings reveal that the N peptide can interact in the same way with both Munc18-1 and Munc18-3 and that the Sx4 N peptide shows little selectivity for Munc18-3.

Strikingly, both Munc18-1 and Munc18-3 form similar monomer–monomer interfaces in the crystal, through the interaction of an extended region of domain 3a (Fig. 2). In addition, the structure of Munc18-1–Sx4 N peptide shows rotation of domain 1, independent of domains 2 and 3 (Fig. 2). Thus, Munc18-1 domain 1 of the B–D complex rotates by 23° around a hinge (residues Ile133–Asn134) with respect to Munc18-1 of the A–C complex. This rotation is unlikely to be associated with N-peptide binding in isolation because the N peptide is present in both Munc18-1 molecules in the crystal structure. A similar domain 1 rotation has been observed previously in the absence of N peptide in the structure of squid Sec1 (squid Munc18, ~65% sequence identity to rat Munc18-1) (17). Domain rotation in both rat Munc18-1 and squid Sec1 structures is likely a result of crystal contacts and would therefore be accessible in the context of the cell, where such rotations may be induced by comparable external forces involving protein or membrane interactions.

**Table 1. Thermodynamic parameters for Munc18–Syntaxin N-peptide interactions**

| Munc18 protein | N-peptide interaction | $\Delta H$, kcal/mol | $\Delta G$, kcal/mol | $K_d$, μM | N |
|---|---|---|---|---|---|
| 1. Munc18-1 | Sx1 (cognate) | −3.8 ± 0.8 | −5.80 ± 0.20 | 58 ± 21 | 0.95 ± 0.49 |
| 2. Munc18-1 | Sx4 (noncognate) | −2.6 ± 0.6 | −6.15 ± 0.12 | 31 ± 8 | 1.10 ± 0.17 |
| 3. Munc18-3 | Sx4 (cognate) | −6.1 ± 1.0 | −7.97 ± 0.07 | 1.5 ± 0.2 | 0.99 ± 0.02 |
| 4. Munc18-3 | Sx1 (noncognate) | −4.3 ± 0.4 | −6.50 ± 0.25 | 18 ± 7 | 1.09 ± 0.09 |

Values are expressed as mean ± SEM for three independent experiments. $K_d$ values are significantly different ($p < 0.05$) except 1:2 and 2:4. See also Fig. S1.

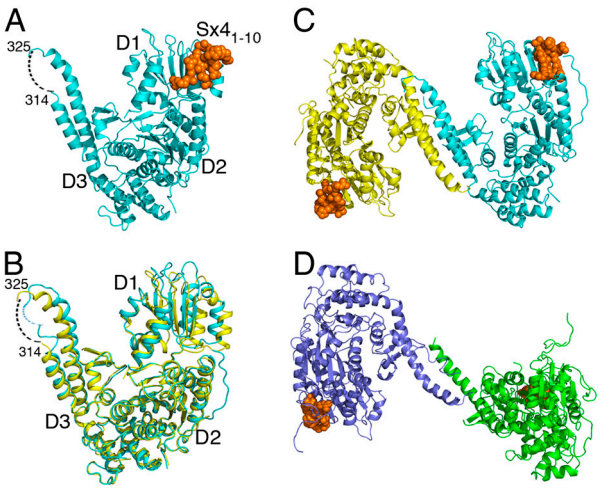


**Fig. 2.** Structure of Munc18-1 complexed with the Sx4 N peptide. (*A*) Ribbon diagram of the structure of Munc18-1 (cyan) bound to the Sx4 N peptide (Sx4$_{1-10}$) (orange). Domains 1, 2, and 3 of Munc18-1 are labeled D1, D2, and D3, respectively. (*B*) Overlay of domains 2 and 3 of the two molecules of Munc18-1 in the asymmetric unit of the crystal structure (cyan, yellow), showing that domain 1 can rotate with respect to domains 2 and 3. (*C*. and *D*) Ribbon diagrams showing that the monomer–monomer interface observed in the crystal structure of (*C*) Munc18-1–Sx4 N peptide (cyan, yellow) resembles that in the crystal structure of (*D*) Munc18-3–Sx4 N peptide (green, purple). Bound Sx4 N peptides are shown in orange space-filling representation.

**N-Peptide Interaction in Munc18-1–Sx1 Closed Complex Is Not Fully Competent.** We also compared the interactions formed between the Sx4 N peptide and Munc18-1 with those formed between the Sx1 N peptide and Munc18-1. For this comparison, we used the crystal structure of Munc18-1 complexed with full-length cytoplasmic closed Sx1 (lacking the C-terminal transmembrane domain), recently revised to include an N-peptide interaction [Protein Data Bank (PDB) ID code 3C98] (5). In this complex, the Sx1 N peptide forms 3 intermolecular hydrogen bonds and 43 VdW interactions with Munc18-1. We investigated whether the reduced number of N-peptide interactions was due to sequence differences between the Sx4 and Sx1 N peptides, but we found this was not the case. The hydrogen bonds in the Munc18-1 complex with the Sx4 N peptide and missing in the complex with the Sx1 N peptide are formed by Arg4, Thr5, and Arg9, and all three residues are conserved in Sx1 and Sx4 N peptides (Fig. S2). Furthermore, far fewer hydrophobic interactions (3 compared with 6–13) are formed between Munc18-1 and the critical Leu8 residue of Sx1 (9) in comparison with the Sx4 N peptide. We therefore conclude, in agreement with Burkhardt et al. (5), that the N-peptide interaction in the Munc18-1–Sx1 crystal structure is not fully competent because of the His tag engineered at the N-terminus of Sx1 and crystal contacts in the region of the N-peptide binding site.

**Domain 3a Conformation.** We have speculated previously (11) that N-peptide binding may be associated with a conformational change in Munc18 or Syntaxin. The availability of two crystal structures of rat Munc18-1—one in the presence of closed Sx1 and the other in the presence of a competent N-peptide interaction—provides an opportunity to investigate whether conformational changes can occur in Munc18-1. We identified a conformational change in Munc18-1 domain 3a (residues 295–358) (Fig. 3, Movie S1); these residues form the predominant interaction site with Sx1 helices H3 and Hc in the Munc18-1–Sx1 closed structure (6). In that structure, Munc18-1 residues 295–358 form a bent hairpin, but in the Munc18-1 structure reported here the hairpin is unfurled, involving a 180° rotation and >25 Å translation of backbone residues to form an extended antiparallel helical hairpin. A similar conformation was observed in the structure of squid Sec1 (17). However, our data show that an SM protein, in this case rat Munc18-1, can access both bent and extended conformations of domain 3a. Importantly, the extended helical hairpin conformation appears to be inconsistent with binding closed Sx1 because it would project directly between the Sx1 Hc:H3 interface (Fig. 3) that defines the closed Sx1 conformation.

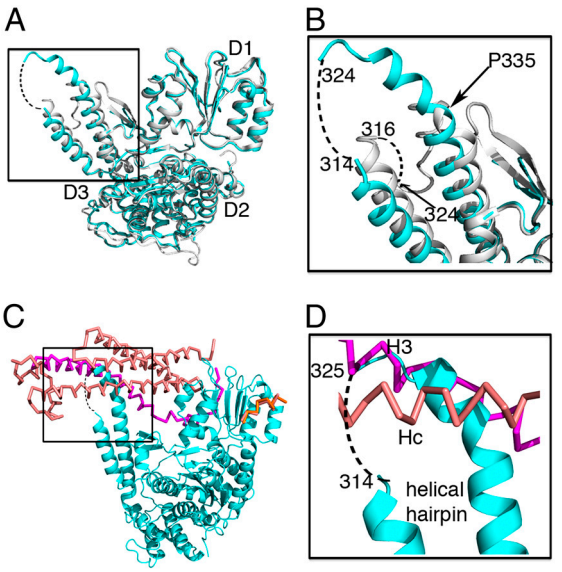


**Fig. 3.** Munc18-1 adopts a conformation that may preclude closed Sx1. (*A*) Superposition of Munc18-1 structures from the complex with Sx4 N peptide (cyan) and the complex with closed Sx1 [3C98 (5), white; for clarity the structure of closed Sx1 has been removed]. (*B*) Close-up of the folded-over helical hairpin of Munc18-1 (white) that is present when closed Sx1 is bound and that is extended (cyan) in the crystal structure of Munc18-1 in the presence of the Sx4 N peptide. Disordered residues in the two Munc18-1 structures are indicated by dotted lines. (*C*) Both *C* and *D* show that the Munc18-1 structure adopted in the complex with Sx4 N peptide may be incompatible with binding closed Sx1. Structures of rat Munc18-1 were superimposed as in *A*; shown are the Munc18-1 structure from the complex with Sx4 N peptide (cyan) and closed Sx1 from the Munc18-1–Sx1 complex [3C98(5); the structure of Munc18-1 has been removed for clarity ]. The helices of Sx1 are shown in salmon (Habc) and pink (SNARE H3). The close-up (*D*) shows that the extended helical hairpin of Munc18-1 protrudes between the Hc–H3 interface (salmon–pink, labeled) and may therefore be incompatible with binding closed Sx1. See also Movie S1.

With the exception of the folded back conformation in rat Munc18-1 bound to closed Sx1, domain 3a is extended in all SM protein crystal structures (Fig. 4*A*). However, it does not always adopt a helical hairpin; in some cases, it forms random coil or strand-like structures. In each case, the conformation is influenced by crystal contacts. In three cases [Munc18-1 and Munc18-3, reported here, and squid Sec1 (17)], a coiled-coil-like interaction is formed between domains 3a from two crystallographically related molecules. Domain 3a variability suggests this region may be unstructured in the unbound solution state and possibly adopts a helical structure upon interaction with partners. It seems unlikely that N-peptide binding to Munc18-1 domain 1 in isolation—that is, in the absence of other Sx1 domains—could induce helical hairpin conformation in domain 3a. However, N-peptide binding is clearly compatible with this domain 3a conformation (Fig. 2).

**Domain 3a May Form Coiled-Coil Interactions.** We analyzed the sequences of domains 3a from Munc18 proteins and found that one of the two helices forming the hairpin has a predicted amphipathic coiled-coil sequence with distinct hydrophobic and basic surfaces (Fig. 4 *B* and *C*). These features suggest the possibility that domain 3a may interact with SNARE proteins and complexes. In the structure of Munc18-1 bound to closed Sx1 (6),

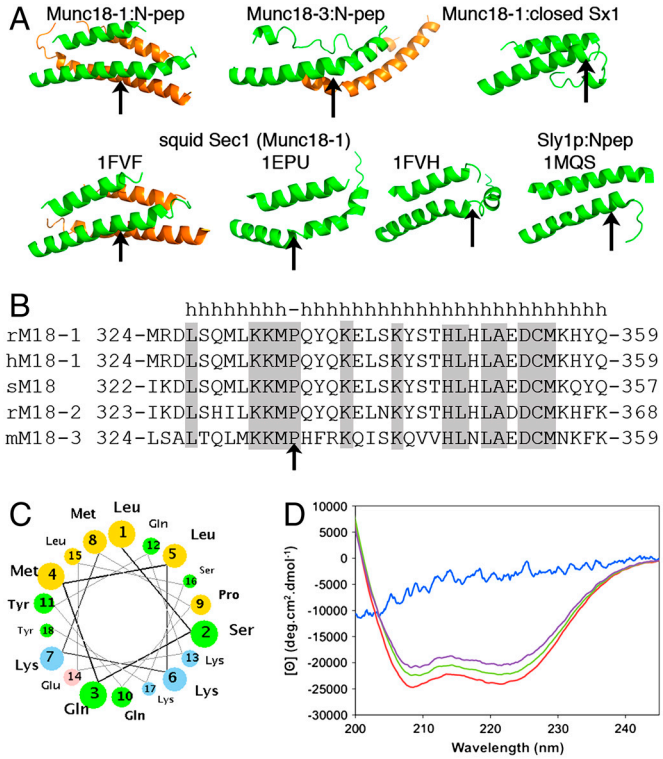


**Fig. 4.** Domain 3a. (*A*) Domains 3a of structurally characterized SM proteins are shown in green. Munc18-1–Sx4 N peptide and rerefined Munc18-3–Sx4 N peptide reported here are in the *Top Left*; other structures are indicated by their name and PDB code. For those structures exhibiting a coiled-coil-like interaction, the crystallographically related domain 3a is shown in orange. Arrows indicate the hinge point (equivalent to P335 of Munc18-1) where domain 3a folds back in the rat Munc18-1 structure bound to closed Sx1, showing that other domain 3a structures are more extended. (*B*) Sequence alignment of domains 3a from Munc18 proteins (rM18-1, rat Munc18-1; hM18-1, human Munc18-1; sM18, squid Sec1; rM18-2, rat Munc18-2; and mM18-3, mouse Munc18-3). Conserved residues are shaded. Helical residues from the structure reported here are indicated by "h." The conserved proline is indicated by an arrow. (*C*) Helical wheel representation of helical residues 327–344 of rat Munc18-1, showing hydrophobic residues in yellow, polar residues in green, acidic residues in pink, and basic residues in blue. (*D*) CD spectra for the domain 3a peptide, residues 326–359 of rat Munc18-1 (blue), SNARE complex (green), and mixture of the peptide and SNARE complex (red). The theoretical curve assuming no interaction between the two is shown in purple.

a strictly conserved proline (P335) in this predicted coiled-coil sequence forms the hinge point of the bent hairpin (Fig. 4*A*). The proline may thus allow the helical hairpin to access both extended and bent conformations.

We used CD spectroscopy to analyze whether a peptide corresponding to this region of Munc18-1 (residues 326–359) could interact with the SNARE ternary complex (formed from Sx1 H3 helix, His-SNAP25, and VAMP2). The CD spectrum from the mixture of peptide and SNARE complex (Fig. 4*D*) reveals an increase in helicity of about 8% in comparison with the SNARE complex. We would expect an increase in helicity of 11% if all 34 peptide residues form coiled-coil interactions with the helical residues of the SNARE complex. These results indicate that the isolated domain 3a peptide interacts with the SNARE complex and that this interaction induces coiled-coil formation in the peptide. Although these data support the conjecture that the domain 3a region of Munc18-1 may be directly involved in SNARE complex interaction, further studies will be needed to confirm this conclusion.

## Discussion

Munc18-1 binds closed Sx1, in an interaction involving Munc18-1 cradling the four-helix bundle of Sx1 (5, 6). This binding mode, which is not universal and does not require an N-peptide interaction, underpins the negative regulation paradigm whereby Munc18-1 inhibits vesicle trafficking by preventing Sx1 forming SNARE complexes (7, 18). The closed binding mode may be important for chaperoning and correctly localizing Sx1 and for preventing ectopic SNARE complex formation (19, 20). Munc18-1 also binds open Sx1 in SNARE complexes, in an interaction that depends on the Sx1 N peptide (9, 10, 19). This second binding mode is associated with the role of Munc18-1 in stimulating SNARE complex formation and vesicle fusion (21, 22), a function that does appear to be conserved across SM protein family members (11, 16, 23). However, the N-peptide binding mode raises an intriguing question—how does a 10-residue peptide enable Munc18-1 to bind open Sx1 in the SNARE complex?

Despite the considerable evidence gathered over recent years showing the importance of the N peptide in Munc18-1–Sx1 interactions (9, 10, 14, 19, 21), our data show that the N peptide is poorly selective; binding affinities and conformations are similar for cognate and noncognate interactions. The most likely explanation for these data is that the N peptide does not act alone. Rather, it may act as a binding tab, a short motif floating free of Sx1 in the SNARE complex allowing Munc18-1 to attach to and probe the complex further. Because the N peptide does not contribute to specificity, this interaction probably precedes a higher specificity, higher affinity interaction with the SNARE complex. Indeed, the Habc and H3 regions of open Sx1 in SNARE complexes have been shown to interact with Munc18-1, supporting the notion that residues other than the N peptide are involved in this interaction (10, 24).

Our results suggest that Sx1 bound to Munc18-1 can form SNARE complexes without apparent inhibition by Munc18-1 or the Sx1 N peptide. Although this finding is supported by some studies (9, 15), it is at odds with the conclusions of others (5), and it will be important to determine the reasons for this discrepancy. Nonetheless, our data support the contention that Munc18-1 can bind an open Sx1 conformation within the SNARE complex when the N peptide is engaged, and this may be facilitated by C-terminal anchoring of Sx1. The crystal structure we report here, together with previously reported structures of SM proteins, suggests how N-peptide binding and a Sx1 C anchor might allow Munc18-1 to bind open Sx1 and thereby enable SNARE complex formation. In the context of the cell, Sx1 is tethered at its C terminus to the plasma membrane, providing an anchor point at the H3 helix. When the Sx1 N peptide binds to domain 1 of Munc18-1, a second anchor point may be made at the N terminus of Sx1. Anchoring of the Sx1 N terminus to domain 1 may enable domain 1 rotation and consequent twisting of Habc away from H3 (Fig. 5,Movie S1, and Movie S2). The Sx1 N peptide and immobilized C terminus may thus provide two anchor points allowing Munc18-1 to bind an open conformation of Sx1 that can then interact with SNARE partners. This assembly may be further stabilized by association of the SNARE complex itself within the Munc18-1 arch previously occupied by the Sx1 closed conformation, as suggested recently by others (15, 25). We emphasize that the model described above is speculative and requires further testing.

Munc18-1 domain 3a may be flexible in the unbound solution state and adopt an ordered conformation upon interaction with binding partners. We showed that a domain 3a peptide interacts with preformed SNARE complex, as evidenced by an increase in helicity consistent with coiled-coil formation. A similar disorder–order transition occurs when SNARE proteins bind partners (26, 27). A role for Munc18-1 domain 3a in SNARE complex formation is supported by recent data showing that mutation of a single Munc18-1 domain 3a residue (Y337) impaired binding to the SNARE complex and inhibited exocytosis but did not affect binary interaction with Sx1 (28). Furthermore, cross-linking

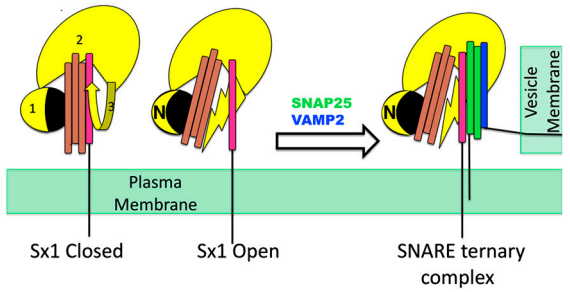


**Fig. 5.** Proposed model of Munc18-1–Sx1a interactions. (*Left*) Closed Sx1 (Habc helices in salmon, SNARE H3 helix in pink) interacts with Munc18-1 (domains 1, 2, and 3 labeled) when the N-peptide binding mode is inactivated; for example, when the N peptide is tagged, Sx1 Ser14 is phosphorylated or the N-peptide binding site of Munc18-1 is blocked. (*Center*) When the N peptide (N) is engaged on domain 1, Munc18-1 can bind open Sx1 possibly through rotation of domain 1 (yellow/black) relative to domains 2 and 3; this may twist Habc away from H3 and allow extension of the Munc18-1 domain 3a helical hairpin, which we propose binds Sx1 H3. See also Movie S2. (*Right*) We propose that the extended domain 3a interacts with SNARE complex.

studies showed that Synaptobrevin (VAMP2) interacts with domain 3a (25).

Perhaps most importantly, our results highlight that there may be many points of intervention, allostery, and control in the Munc18-1:Sx1 interaction. Potential target points additional to the open–closed transition of Sx1 include Sx1 N peptide, Sx1 C-terminal anchor, Munc18-1 N-peptide binding site, Munc18-1 domain 1 rotation, and Munc18-1 domain 3a conformational switching. Upstream regulatory factors might thereby control fusion by modifying any one or more of these sites. Indeed, this model is consistent with recent data showing that phosphorylation of Sx1 at Ser14 near the N peptide inhibits exocytosis (29); that the binding site of the Munc18-1 interacting protein MINT1 overlaps with that of the Sx1 N peptide (20); and that PKC phosphorylation sites on Munc18-1 (Ser306 and Ser313) (30) are located on domain 3a.

In summary, our model for SNARE complex formation suggests important roles for Munc18-1 domain 3a, the Sx1 N peptide, and the Sx1 C-terminal anchor.

## Materials and Methods

Peptides corresponding to the N-terminal 10 residues (N peptides) of Sx1 (MKDRTQELRT), Sx4 (MRDRTHELRQ), and a coiled-coil sequence of rat Munc18-1 domain 3a (residues 326–359) were purchased (Auspep).

**ITC.** For ITC, N-terminally His-tagged Munc18-3 was produced as described previously (31). A pET28 vector encoding C-terminally His-tagged Munc18-1 was kindly donated by Jingshi Shen. Munc18-1 was expressed in *Escherichia coli*; for purification protocol see *SI Materials and Methods*. ITC experiments were carried out at 298 K using an iTC200 (Microcal). The proteins were in 62 mM HEPES pH 7, with 150 mM NaCl and 1 mM 2-mercaptoethanol (β-ME). Stock solutions of Sx4 and Sx1 N peptides at 7.5 mM were prepared in the same buffer. Munc18-1 or Munc18-3 at 35–50 μM were titrated with 400–1700 μM of the N peptides. Injection volumes of 2.2 μL were used for the titrations. The heat released was measured and integrated using Microcal ORIGIN 7.0 software to calculate stoichiometry (N), equilibrium constant $K_a (= 1/K_d)$, and binding enthalpy ($\Delta H$) of the interactions. Binding parameters from three different experiments were averaged to give standard error of the mean (SEM), and unpaired Student's *t*-tests were used to assess whether $K_d$ values were statistically different at $p < 0.05$ (Table 1). The relatively large errors in $K_d$ values are a consequence of performing the experiments, by necessity, at nonideal Wiseman *c* values ($c = [\text{Munc18}]/K_d$) (32). Raw data are provided in Fig. S1.

**Munc18-1–SNARE Interactions.** Rat Sx1 (residues 1–261) and Sx1 H3 SNARE motif (residues 180–261) were subcloned into pET20b encoding a C-terminal hexa-histidine tag. We used a codon-optimized synthetic gene of rat Sx1 (GeneArt). Purification procedures are given in *SI Materials and Methods*. Production of N-terminally tagged GST-VAMP2 (Synaptobrevin) (residues 1–94) has been described previously, as has the procedure to remove the GST tag from VAMP2 (16, 22). SNAP25 (residues 1–206) was subcloned into pMCSG7 encoding an N-terminal His tag and a tobacco etch virus (TEV) cleavage site. His-SNAP25 was purified on PrepEase resin followed by size exclusion chromatography. To remove the His tag, resin-purified His-SNAP25 was incubated at 4 °C overnight with His-tagged TEV protease. The protease was removed with $Co^{2+}$-affinity beads, and SNAP25 was further purified by size exclusion chromatography.

Sx1-His alone or mixed with purified detagged Munc18-1 was immobilized on $Co^{2+}$-affinity beads for 2 h at 4 °C (Munc18-1 was prepared as described in *SI Materials and Methods* for crystallization experiments). Beads with immobilized Sx1-His or Munc18-1–Sx1-His were then incubated overnight at 4 °C with SNAP25 and VAMP2 in binding buffer containing 25 mM Tris-HCl, pH 7.5, 150 mM NaCl, 10% glycerol, 5 mM imidazole, 2 mM β-ME, and 0.1% Triton-X100. For binding of Munc18-1 to preformed SNARE complex, the SNARE complex (Sx1-His/SNAP25/VAMP2) was first assembled on beads as described above and then incubated overnight at 4 °C with Munc18-1. In each case, beads were washed extensively with binding buffer, eluted with binding buffer containing 200 mM imidazole and bound proteins analyzed by SDS-PAGE and Coomassie Blue.

See *SI Materials and Methods* for additional materials and methods information.

**ACKNOWLEDGMENTS.** We thank Jingshi Shen for the Munc18-1–His clone, Fred Meunier for critical comment, and the Australian National Health and Medical Research Council (NHMRC) for financial support (Grants 401643 and 535921). J.L.M. is an Australian Research Council Laureate Fellow and Honorary NHMRC Fellow; B.M.C. holds an NHMRC Career Development Award. We acknowledge use of the University of Queensland Remote Operation Crystallization and X-ray Diffraction Facility and thank Karl Byriel and Gordon King for assistance. X-ray data were measured on the MX2 beamline at the Australian Synchrotron, Victoria, Australia.

1. Jahn R, Scheller RH (2006) SNAREs—Engines for membrane fusion. *Nat Rev Mol Cell Biol* 7:631–643.
2. Südhof T, Rothman J (2009) Membrane fusion: Grappling with SNARE and SM proteins. *Science* 323:474–477.
3. Toonen RF, Verhage M (2007) Munc18-1 in secretion: Lonely Munc joins SNARE team and takes control. *Trends Neurosci* 30:564–572.
4. Rizo J, Rosenmund C (2008) Synaptic vesicle fusion. *Nat Struct Mol Biol* 15:665–674.
5. Burkhardt P, Hattendorf DA, Weis WI, Fasshauer D (2008) Munc18a controls SNARE assembly through its interactions with the syntaxin N-peptide. *EMBO J* 27:923–933.
6. Misura KM, Scheller RH, Weis WI (2000) Three-dimensional structure of the neuronal-Sec1-syntaxin 1a complex. *Nature* 404:355–362.
7. Dulubova I, et al. (1999) A conformational switch in syntaxin during exocytosis: Role of Munc18. *EMBO J* 18:4372–4382.
8. Gerber S, et al. (2008) Conformational switch of syntaxin-1 controls synaptic vesicle fusion. *Science* 321:1507–1510.
9. Shen J, Tareste DC, Paumet F, Rothman JE, Melia TJ (2007) Selective activation of cognate SNAREpins by Sec1/Munc18c (SM) proteins. *Cell* 128:1–13.
10. Dulubova I, et al. (2007) Munc18-1 binds directly to the neuronal SNARE complex. *Proc Natl Acad Sci USA* 104:2697–2702.
11. Hu S-H, Latham CF, Gee CL, James DE, Martin JL (2007) Structure of the Munc18c/Syntaxin4 N-peptide complex defines universal features of the N-peptide binding mode of Sec1/Munc18 proteins. *Proc Natl Acad Sci USA* 104:8773–8778.
12. Bryant NJ, Govers R, James DE (2002) Regulated transport of the glucose transporter GLUT4. *Mol Cell Biol* 3:267–277.
13. Tellam JT, et al. (1997) Characterization of Munc-18c and syntaxin-4 in 3T3-L1 adipocytes. *J Biol Chem* 272:6179–6186.
14. Khvotchev M, et al. (2007) Dual modes of Munc18-1/SNARE interactions are coupled by functionally critical binding to syntaxin-1 N terminus. *J Neurosci* 27:12147–12155.
15. Shen J, Rathore SS, Khandan L, Rothman JE (2010) SNARE bundle and syntaxin N-peptide constitute a minimal complement for Munc18-1 activation of membrane fusion. *J Cell Biol* 190:55–63.
16. Latham CF, et al. (2006) Molecular dissection of the Munc18c/Syntaxin4 interaction: Implications for regulation of membrane trafficking. *Traffic* 7:1408–1419.
17. Bracher A, Weissenhorn W (2001) Crystal structure of neuronal squid sec1 implicate inter-domain hinge movement in the release of t-SNAREs. *J Mol Biol* 306:7–13.
18. Yang B, Steegmaier M, Gonzalez LJ, Scheller R (2000) nSec1 binds a closed conformation of syntaxin1A. *J Cell Biol* 148:247–252.
19. Rickman C, Medine CN, Bergmann A, Duncan RR (2007) Functionally and spatially distinct modes of Munc18-Syntaxin 1 interaction. *J Biol Chem* 282:12097–12103.
20. Han L, et al. (2009) Rescue of Munc18-1 and -2 double knockdown reveals the essential functions of interaction between Munc18 and closed syntaxin in PC12 cells. *Mol Biol Cell* 20:4962–4975.
21. Zilly FE, Sorensen JB, Jahn R, Lang T (2006) Munc18-bound Syntaxin readily forms SNARE complexes with synaptobrevin in native plasma membranes. *PLoS Biol* 4:1789–1792.

22. Malintan NT, et al. (2009) Abrogating Munc18-1 SNARE complex interaction has limited impact on exocytosis in PC12 cells. *J Biol Chem* 284:20840–20847.
23. Bracher A, Weissenhorn W (2002) Structural basis for the Golgi membrane recruitment of Sly1p by Sed5p. *EMBO J* 21:6114–6124.
24. Rodkey TL, Liu S, Barry M, McNew JA (2008) Munc18a scaffolds SNARE assembly to promote membrane fusion. *Mol Biol Cell* 19:5422–5434.
25. Xu Y, Su L, Rizo J (2010) Binding of Munc18-1 to synaptobrevin and to the SNARE four-helix bundle. *Biochemistry* 49:1568–1576.
26. Fasshauer D, Antonin W, Margittai M, Pabst S, Jahn R (1999) Mixed and non-cognate SNARE complexes. Characterization of assembly and biophysical properties. *J Biol Chem* 274:15440–15446.
27. Ellena JF, et al. (2009) Dynamic structure of lipid-bound synaptobrevin suggests a nucleation-propagation mechanism for trans-SNARE complex formation. *Proc Natl Acad Sci USA* 106:20306–20311.
28. Boyd A, et al. (2008) A random mutagenesis approach to isolate dominant-negative yeast sec1 mutants reveals a functional role for domain 3a in yeast and mammalian Sec1/Munc18 proteins. *Genetics* 180:165–178.
29. Rickman C, Duncan RR (2010) Munc18/Syntaxin interaction kinetics control secretory vesicle dynamics. *J Biol Chem* 285:3965–3972.
30. Barclay JW, et al. (2003) Phosphorylation of Munc18 by protein kinase C regulates the kinetics of exocytosis. *J Biol Chem* 278:10538–10545.
31. Hu S-H, et al. (2003) Recombinant expression of Munc18c in a baculovirus system and interaction with Syntaxin4. *Protein Expres Purif* 31:305–310.
32. Wiseman T, Williston S, Brandts JF, Lin LN (1989) Rapid measurement of binding constants and heats of binding using a new titration calorimeter. *Anal Biochem* 179:131–137.